BNL-209087-2018-TECH

CBETA/021

Comprehensive tracking study for the H-dipoles and common magnets in the splitter sections of the Cornell/Brookhaven Energy-Recovery-Linac Test Accelerator

R. Bass, S. Peggs

August 2017

Collider Accelerator Department

Brookhaven National Laboratory

U.S. Department of Energy

USDOE Office of Science (SC), Nuclear Physics (NP) (SC-26)

DISCLAIMER

Comprehensive Tracking Study for the H-Dipoles and Common Magnets in the Splitter Sections of the Cornell/Brookhaven Energy-Recovery-Linac Test Accelerator

Rachel Bass
Grinnell College
Mentor: Jim Crittenden
Cornell University, CLASSE

August 10, 2017

Abstract

The Cornell-Brookhaven Energy-Recovery-Linac Test Accelerator will have two splitter sections responsible for and guiding beams of 42, 78, 114, and 150 MeV energies between the Fixed-Field Alternating Gradient return loop and the Main Linac Cryomodule [6], correcting optics, and providing path length adjustments. Modeling of all 36 H-dipole magnets under contract with Elytt Energy has been completed. Four common dipoles, two of which are needed for next year's Fractional Arc Test, will be added to the order with Elytt. The design of these magnets is underway. This report describes the findings of the tracking studies of the 36 H-dipoles and gives the status of the common dipoles.

1 Introduction

The Cornell-Brookhaven Energy-Recovery-Linac Test Accelerator (CBETA) will be the first multi-pass ERL using superconducting radiofrequency cavities and a non-scaling Fixed-Field Alternating Gradient (FFAG) return loop. This accelerator will be used as proof of concept for the proposed construction of eRHIC at Brookhaven National Laboratory as well as for conducting scientific experiments. Beyond accelerator physics, the brightness of the 150 MeV beam lends itself to X-ray and nuclear physics applications. [5]

The two splitter regions of CBETA are responsible for providing the path length adjustments of each beam needed for energy recovery. Consequently, each magnet in the splitter regions must be carefully designed and modeled. The design process required an open and frequently used line of communication between Elytt Energy in Madrid and the CBETA team at Cornell. The basic design of the 36 H-dipoles was established on July 18. The

design specifications for the splitter H-dipoles are met using a total of two coil lengths, three steel lengths, and four removable chamfer insert designs.

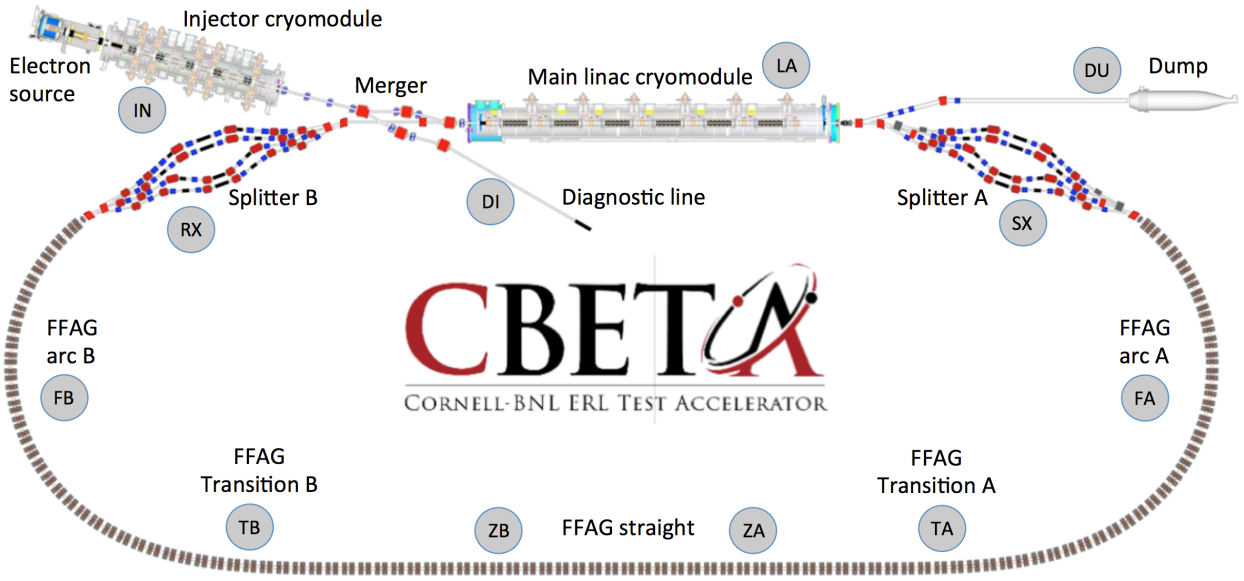

Fig. 1: Complete CBETA layout. SX and RX splitter sections are upstream and downstream of the MLC, respectively.

The common dipoles present a design challenge as they are responsible for transitioning the four beams between the Main Linac Cryomodule (MLC) and splitters as well as between the splitters and FFAG return loop. These dipoles get their name because they are common to the four beam energies, not the four locations. There are additional constraints unique to individual magnet locations as well. The design of a common dipole that will satisfy requirements in all four locations is underway and initial findings are promising. Elytt will be responsible for the engineering and manufacturing of these dipoles.

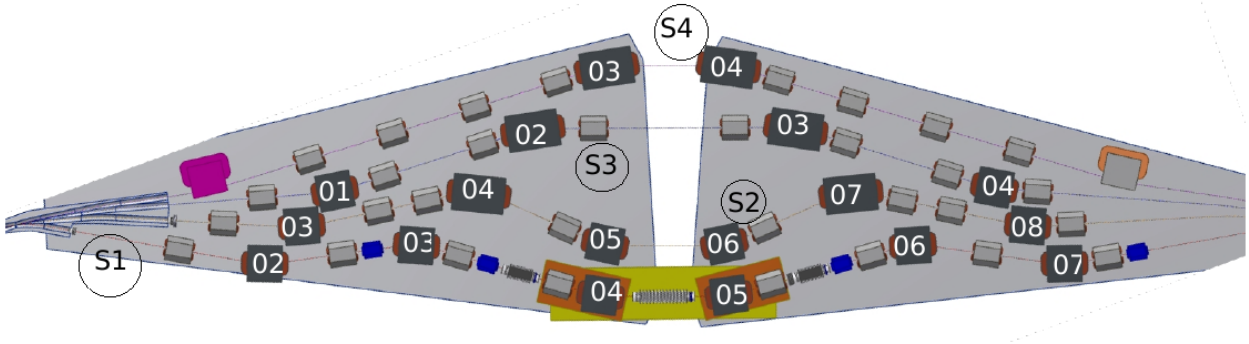

Fig. 2: SX splitter section. Each H-dipole is labeled; common dipoles S1.BEN01 and S1.BEN08 are not shown. The RX splitter is similarly laid out. The light gray magnets are quadrupoles, and the blue magnets are vertical correctors, of which four of sixteen are shown. Four additional small steering magnets are not shown.

2 Modeling and Data Visualization

In order to complete this study, every dipole needed to be studied to ensure that it has an acceptable region of bend angle uniformity and will perform as needed. The success of CBETA will rely on careful engineering and precise manufacturing; consequently, accurate magnet model performance and agreement with Elytt's models are taken as two indicators that the H-dipoles will function as needed. Due to the symmetry between the two splitter sections (see Fig. 1) and within the splitter itself (see Fig. 2), one model was sometimes be used for multiple locations. Using the field integral values found in Tables 1 and 2, the activation current necessary to achieve the desired bend angle was calculated for each dipole. The tracking study itself was a two-part process described in Sections 2.1 and 2.2.
Table 1: Design values for magnets used in one-pass operation. Note that S1.BEN61-64 are in the same location as S1.BEN03-6. The field integral values are used to calculate the necessary excitation current. Bend angles were rounded to three significant figures in the post-processor scripts.

splitter_magnets_1pass_20170410.table.txt Mon Aug 07 13:31:25 2017 1

	Type	S Position (m)	Length (m)	Momentum (MeV)	B field (T)	B integral (T-m)	Bd angle (degrees)	Bd Radius (m)	Sagitta (cm)	Gradient (T/m)	L (mH)	NI kA-turns	Power Supply (V)	(A)	Curr Density A/mm^2
1	S1.BEN01 H-common	23.150	0.160	41.997	-0.393	-0.079	32.487	0.283	1.127	0.000	47.10	-5.91	-6.1	-113.7	-4.92
2	S1.BEN02 H-dip-1	24.471	0.160	41.997	0.243	0.044	-17.991	-0.510	-0.627	0.000	20.00	3.62	3.2	69.7	3.01
3	S1.BEN61 H-dip-1	25.331	0.160	41.997	-0.257	-0.047	19.022	0.482	0.662	0.000	20.00	-3.83	-3.4	-73.7	-3.19
4	S1.BEN62 H-dip-1	26.508	0.160	41.997	0.149	0.027	-11.001	-0.831	-0.385	0.000	20.00	2.22	2.0	42.7	1.85
5	S1.BEN63 H-dip-1	27.308	0.160	41.997	0.149	0.027	-11.001	-0.831	-0.385	0.000	20.00	2.22	2.0	42.7	1.85
6	S1.BEN64 H-dip-1	28.486	0.160	41.997	-0.257	-0.047	19.022	0.482	0.662	0.000	20.00	-3.83	-3.4	-73.7	-3.19
7	S1.BEN07 H-dip-1	29.346	0.160	41.997	0.243	0.044	-17.991	-0.510	-0.627	0.000	20.00	3.62	3.2	69.7	3.01
8	S1.BEN08 H-common	30.676	0.160	41.997	-0.363	-0.073	30.023	0.306	1.043	0.000	47.10	-5.46	-5.6	-104.9	-4.54
9	S1.QUA01 Quad-A	23.971	0.150	41.997	0.000	0.000	0.000	0.000	0.000	-0.999	0.44	-0.20	-1.1	-2.5	-0.52
10	S1.QUA02 Quad-A	24.921	0.150	41.997	0.000	0.000	0.000	0.000	0.000	1.866	0.44	0.38	2.0	4.6	0.97
11	S1.QUA03 Quad-A	25.581	0.150	41.997	0.000	0.000	0.000	0.000	0.000	-1.110	0.44	-0.23	-1.2	-2.8	-0.57
12	S1.QUA04 Quad-A	26.258	0.150	41.997	0.000	0.000	0.000	0.000	0.000	0.666	0.44	0.14	0.7	1.7	0.34
13	S1.QUA05 Quad-W	27.558	0.150	41.997	0.000	0.000	0.000	0.000	0.000	3.258	0.44	0.66	0.7	60.2	2.61
14	S1.QUA06 Quad-A	28.236	0.150	41.997	0.000	0.000	0.000	0.000	0.000	-1.894	0.44	-0.39	-2.0	-4.7	-0.98
15	S1.QUA07 Quad-A	28.896	0.150	41.997	0.000	0.000	0.000	0.000	0.000	2.154	0.44	0.44	2.3	5.3	1.11
16	S1.QUA08 Quad-A	29.846	0.150	41.997	0.000	0.000	0.000	0.000	0.000	-0.773	0.44	-0.16	-0.8	-1.9	-0.40
17	R1.BEN08 H-common	79.644	0.160	41.997	-0.363	-0.073	30.023	0.306	1.043	0.000	47.10	-5.46	-5.6	-104.9	-4.54
18	R1.BEN07 H-dip-1	80.964	0.160	41.997	0.243	0.044	-17.991	-0.510	-0.627	0.000	20.00	3.62	3.2	69.7	3.01
19	R1.BEN64 H-dip-1	81.824	0.160	41.997	-0.257	-0.047	19.022	0.482	0.662	0.000	20.00	-3.83	-3.4	-73.7	-3.19
20	R1.BEN63 H-dip-1	83.001	0.160	41.997	0.149	0.027	-11.001	-0.831	-0.385	0.000	20.00	2.22	2.0	42.7	1.85
21	R1.BEN62 H-dip-1	83.851	0.160	41.997	0.149	0.027	-11.001	-0.831	-0.385	0.000	20.00	2.22	2.0	42.7	1.85
22	R1.BEN61 H-dip-1	85.029	0.160	41.997	-0.257	-0.047	19.022	0.482	0.662	0.000	20.00	-3.83	-3.4	-73.7	-3.19
23	R1.BEN02 H-dip-1	85.889	0.160	41.997	0.243	0.044	-17.991	-0.510	-0.627	0.000	20.00	3.62	3.2	69.7	3.01
24	R1.BEN01 H-common	87.218	0.160	41.997	-0.363	-0.073	30.023	0.306	1.043	0.000	47.10	-5.46	-5.6	-104.9	-4.54
25	R1.BEN99 H-dip-1	89.406	0.160	41.997	-0.029	-0.005	2.120	4.342	0.074	0.000	20.00	-0.43	-0.4	-8.2	-0.35
26	R1.QUA08 Quad-A	80.464	0.150	41.997	0.000	0.000	0.000	0.000	0.000	0.197	0.44	0.04	0.2	0.5	0.10
27	R1.QUA07 Quad-A	81.414	0.150	41.997	0.000	0.000	0.000	0.000	0.000	1.540	0.44	0.31	1.6	3.8	0.80
28	R1.QUA06 Quad-A	82.074	0.150	41.997	0.000	0.000	0.000	0.000	0.000	-1.767	0.44	-0.36	-1.9	-4.4	-0.91
29	R1.QUA05 Quad-W	82.751	0.150	41.997	0.000	0.000	0.000	0.000	0.000	2.930	0.44	0.60	0.7	54.2	2.34
30	R1.QUA04 Quad-A	84.101	0.150	41.997	0.000	0.000	0.000	0.000	0.000	0.850	0.44	0.17	0.9	2.1	0.44
31	R1.QUA03 Quad-A	84.779	0.150	41.997	0.000	0.000	0.000	0.000	0.000	-1.143	0.44	-0.23	-1.2	-2.8	-0.59
32	R1.QUA02 Quad-A	85.439	0.150	41.997	0.000	0.000	0.000	0.000	0.000	2.042	0.44	0.42	2.2	5.1	1.06
33	R1.QUA01 Quad-A	86.389	0.150	41.997	0.000	0.000	0.000	0.000	0.000	-0.938	0.44	-0.19	-1.0	-2.3	-0.49
		(m)	(m)	(MeV)	(T)	(T-m)	(degrees)	(m)	(cm)	(T/m)	(mH)	kA-turns	(V)	(A)	A/mm^2
	Type	S-Position	Length	Momentum	B-field	B integral	Bd angle	Bd Radius	Sagitta	Gradient	L	NI	Power-Supply		Curr-Density

Table 2: Design values for dipoles in four-pass operation. The field integral values are used to calculate the necessary excitation current. Bend angles were rounded to three significant figures in the post-processor scripts.

splitter_magnets_4pass_20170410.table.txt Mon Aug 07 12:13:03 2017 1

	Type	S Position (m)	Length (m)	Momentum (MeV)	B field (T)	B integral (T-m)	Bd angle (degrees)	Bd Radius (m)	Sagitta (cm)	Gradient (T/m)	L (mH)	NI kA-turns	Power Supply (V)	Power Supply (A)	Curr Density A/mm^2
1	S1.BEN01 H-common	23.150	0.160	41.997	-0.393	-0.079	32.487	0.283	1.127	0.000	47.10	-5.91	-6.1	-113.7	-4.92
2	S1.BEN02 H-dip-1	24.471	0.160	41.997	0.243	0.044	-17.991	-0.510	-0.627	0.000	20.00	3.62	3.2	69.7	3.01
3	S1.BEN03 H-dip-1	25.331	0.160	41.997	-0.338	-0.061	24.981	0.366	0.870	0.000	20.00	-5.03	-4.4	-96.8	-4.19
4	S1.BEN04 H-dip-1	26.537	0.160	41.997	0.230	0.042	-17.017	-0.539	-0.592	0.000	20.00	3.42	3.0	65.8	2.85
5	S1.BEN05 H-dip-1	27.337	0.160	41.997	0.230	0.042	-17.017	-0.539	-0.592	0.000	20.00	3.42	3.0	65.8	2.85
6	S1.BEN06 H-dip-1	28.544	0.160	41.997	-0.338	-0.061	24.981	0.366	0.870	0.000	20.00	-5.03	-4.4	-96.8	-4.19
7	S1.BEN07 H-dip-1	29.404	0.160	41.997	0.243	0.044	-17.991	-0.510	-0.627	0.000	20.00	3.62	3.2	69.7	3.01
8	S1.BEN08 H-common	30.733	0.160	41.997	-0.363	-0.073	30.023	0.306	1.043	0.000	47.10	-5.46	-5.6	-104.9	-4.54
17	R1.BEN08 H-common	79.701	0.160	41.997	-0.363	-0.073	30.023	0.306	1.043	0.000	47.10	-5.46	-5.6	-104.9	-4.54
18	R1.BEN07 H-dip-1	81.021	0.160	41.997	0.243	0.044	-17.991	-0.510	-0.627	0.000	20.00	3.62	3.2	69.7	3.01
19	R1.BEN06 H-dip-1	81.881	0.160	41.997	-0.338	-0.061	24.981	0.366	0.870	0.000	20.00	-5.03	-4.4	-96.8	-4.19
20	R1.BEN05 H-dip-1	83.088	0.160	41.997	0.230	0.042	-17.017	-0.539	-0.592	0.000	20.00	3.42	3.0	65.8	2.85
21	R1.BEN04 H-dip-1	83.938	0.160	41.997	0.230	0.042	-17.017	-0.539	-0.592	0.000	20.00	3.42	3.0	65.8	2.85
22	R1.BEN03 H-dip-1	85.144	0.160	41.997	-0.338	-0.061	24.981	0.366	0.870	0.000	20.00	-5.03	-4.4	-96.8	-4.19
23	R1.BEN02 H-dip-1	86.004	0.160	41.997	0.243	0.044	-17.991	-0.510	-0.627	0.000	20.00	3.62	3.2	69.7	3.01
24	R1.BEN01 H-common	87.334	0.160	41.997	-0.363	-0.073	30.023	0.306	1.043	0.000	47.10	-5.46	-5.6	-104.9	-4.54
33	S2.BEN01 Septum-1	102.643	0.200	77.998	-0.168	-0.034	7.391	1.552	0.322	0.000	0.00	0.00	0.0	0.0	0.00
34	S2.BEN02 H-dip-4	103.093	0.100	77.998	-0.070	-0.009	2.005	2.865	0.043	0.000	6.40	-1.03	-1.1	-17.2	-0.69
35	S2.BEN03 H-dip-1	103.723	0.160	77.998	0.452	0.082	-17.991	-0.510	-0.627	0.000	20.00	6.73	5.9	129.4	5.60
36	S2.BEN04 H-dip-2	104.770	0.240	77.998	-0.655	-0.168	37.013	0.372	1.921	0.000	27.60	-9.67	-12.3	-185.9	-8.04
37	S2.BEN05 H-dip-1	105.657	0.160	77.998	0.602	0.109	-24.007	-0.382	-0.834	0.000	20.00	8.97	7.9	172.5	7.46
38	S2.BEN06 H-dip-1	106.337	0.160	77.998	0.602	0.109	-24.007	-0.382	-0.834	0.000	20.00	8.97	7.9	172.5	7.46
39	S2.BEN07 H-dip-2	107.324	0.240	77.998	-0.651	-0.167	36.784	0.374	1.909	0.000	27.60	-9.61	-12.2	-184.7	-7.99
40	S2.BEN08 H-dip-1	108.272	0.160	77.998	0.442	0.080	-17.647	-0.520	-0.614	0.000	20.00	6.59	5.8	126.7	5.48
41	S2.BEN09 H-dip-4	108.852	0.100	77.998	-0.070	-0.009	2.005	2.865	0.043	0.000	6.40	-1.03	-1.1	-17.2	-0.69
42	S2.BEN10 Septum-1	109.352	0.200	77.998	-0.168	-0.034	7.391	1.552	0.322	0.000	0.00	0.00	0.0	0.0	0.00
51	R2.BEN10 Septum-1	159.235	0.200	77.998	-0.168	-0.034	7.391	1.552	0.322	0.000	0.00	0.00	0.0	0.0	0.00
52	R2.BEN09 H-dip-4	159.685	0.100	77.998	-0.070	-0.009	2.018	2.865	0.044	0.000	6.40	-1.03	-1.1	-17.2	-0.69
53	R2.BEN08 H-dip-1	160.315	0.160	77.998	0.399	0.072	-15.904	-0.577	-0.555	0.000	20.00	5.94	5.2	114.3	4.94
54	R2.BEN07 H-dip-2	161.356	0.240	77.998	-0.629	-0.161	35.545	0.387	1.848	0.000	27.60	-9.28	-11.8	-178.5	-7.72
55	R2.BEN06 H-dip-1	162.268	0.160	77.998	0.602	0.109	-24.030	-0.382	-0.836	0.000	20.00	8.97	7.9	172.5	7.46
56	R2.BEN05 H-dip-1	162.956	0.160	77.998	0.602	0.109	-24.030	-0.382	-0.836	0.000	20.00	8.97	7.9	172.5	7.46
57	R2.BEN04 H-dip-2	163.968	0.240	77.998	-0.655	-0.168	36.972	0.372	1.919	0.000	27.60	-9.67	-12.3	-185.9	-8.04
58	R2.BEN03 H-dip-1	164.916	0.160	77.998	0.451	0.082	-17.987	-0.510	-0.627	0.000	20.00	6.73	5.9	129.4	5.60
59	R2.BEN02 H-dip-4	165.496	0.100	77.998	-0.070	-0.009	2.005	2.865	0.043	0.000	6.40	-1.03	-1.1	-17.2	-0.69
60	R2.BEN01 Septum-1	165.996	0.200	77.998	-0.168	-0.034	7.391	1.552	0.322	0.000	0.00	0.00	0.0	0.0	0.00
69	S3.BEN01 H-dip-1	183.051	0.160	113.999	0.574	0.104	-15.642	-0.586	-0.546	0.000	20.00	8.56	7.5	164.5	7.12
70	S3.BEN02 H-dip-3	184.466	0.310	113.999	-0.424	-0.133	19.996	0.888	1.350	0.000	34.00	-6.28	-8.0	-120.8	-5.22
71	S3.BEN03 H-dip-3	185.883	0.310	113.999	-0.424	-0.133	19.996	0.888	1.350	0.000	34.00	-6.28	-8.0	-120.8	-5.22
72	S3.BEN04 H-dip-1	187.167	0.160	113.999	0.574	0.104	-15.642	-0.586	-0.546	0.000	20.00	8.55	7.5	164.5	7.11
81	R3.BEN04 H-dip-1	239.617	0.160	113.999	0.568	0.103	-15.487	-0.591	-0.539	0.000	20.00	8.47	7.5	162.8	7.04
82	R3.BEN03 H-dip-3	240.974	0.310	113.999	-0.424	-0.133	19.978	0.888	1.346	0.000	34.00	-6.28	-8.0	-120.8	-5.22
83	R3.BEN02 H-dip-3	242.440	0.310	113.999	-0.424	-0.133	19.978	0.888	1.346	0.000	34.00	-6.28	-8.0	-120.8	-5.22
84	R3.BEN01 H-dip-1	243.786	0.160	113.999	0.577	0.104	-15.696	-0.583	-0.546	0.000	20.00	8.59	7.6	165.2	7.15
93	S4.BEN01 Septum-2	261.550	0.120	149.999	0.393	0.079	-8.995	-0.764	-0.235	0.000	0.00	0.00	0.0	0.0	0.00
94	S4.BEN02 H-dip-4	262.321	0.100	149.999	0.464	0.060	-6.875	-0.831	-0.150	0.000	6.40	6.85	7.2	114.1	4.56
95	S4.BEN03 H-dip-3	263.555	0.310	149.999	-0.670	-0.210	24.007	0.740	1.617	0.000	34.00	-9.92	-12.6	-190.7	-8.25
96	S4.BEN04 H-dip-3	265.107	0.310	149.999	-0.670	-0.210	24.007	0.740	1.617	0.000	34.00	-9.92	-12.6	-190.7	-8.25
97	S4.BEN05 H-dip-4	266.157	0.100	149.999	0.461	0.060	-6.875	-0.836	-0.149	0.000	6.40	6.80	7.2	113.4	4.54
98	S4.BEN06 Septum-2	266.928	0.120	149.999	0.393	0.079	-8.995	-0.764	-0.235	0.000	0.00	0.00	0.0	0.0	0.00
107	R4.BEN06 Septum-2	318.231	0.120	149.999	0.393	0.065	-7.448	-0.926	-0.194	0.000	0.00	0.00	0.0	0.0	0.00
108	R4.BEN05 H-dip-4	319.002	0.100	149.999	0.479	0.062	-7.153	-0.804	-0.157	0.000	6.40	7.08	7.5	118.0	4.72
109	R4.BEN04 H-dip-3	320.159	0.310	149.999	-0.670	-0.210	23.999	0.740	1.617	0.000	34.00	-9.92	-12.6	-190.7	-8.25
110	R4.BEN03 H-dip-3	321.731	0.310	149.999	-0.670	-0.210	23.999	0.740	1.617	0.000	34.00	-9.92	-12.6	-190.7	-8.25
111	R4.BEN02 H-dip-4	322.892	0.100	149.999	0.469	0.061	-6.945	-0.822	-0.151	0.000	6.40	6.93	7.3	115.4	4.62
112	R4.BEN01 Septum-2	323.663	0.120	149.999	0.393	0.079	-8.995	-0.764	-0.235	0.000	0.00	0.00	0.0	0.0	0.00
		(m)	(m)	(MeV)	(T)	(T-m)	(degrees)	(m)	(cm)	(T/m)	(mH)	kA-turns	(V)	(A)	A/mm^2
	Type	S-Position	Length	Momentum	B-field	B integral	Bd angle	Bd Radius	Sagitta	Gradient	L	NI	Power-Supply		Curr-Density

2.1 OPERA Modeling and Post-Processing Streamlined

First, the magnet had to be modeled using OPERA simulation software [3]. In order to streamline the process, the scripts used to build the model and perform post-processing analysis were refined so that minimal changes needed to be made when switching between magnet models. After a model is completed, two post-processing scripts are executed. The first is responsible for calculating the field integral and producing the data needed for the field integral uniformity plots seen in Figures 5 and 6. The second script is used for the tracking calculations needed to create the bend angle uniformity plots seen in Figures 7 and 8. Once modeling and post-processing are completed in OPERA, images like the one in Figure 3 can be viewed. These images help visualize a beam's path through a dipole at different entrance locations along the magnet's transverse axis. The individual paths a beam could take through the dipole are better visualized using the Physics Analysis Workstation (`PAW`) [4].

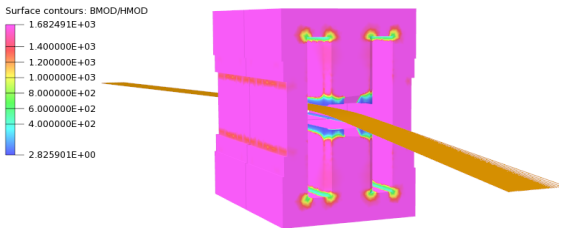

Fig. 3: R3.BEN03/4 H-dipole design with beam tracking of 150 MeV electrons. This image shows contours of magnetic permeability. The high permeability in the pink regions shows that the steel is not near saturation. The asymmetrical chamfer can be seen in purple between the blue regions above and below the beam.

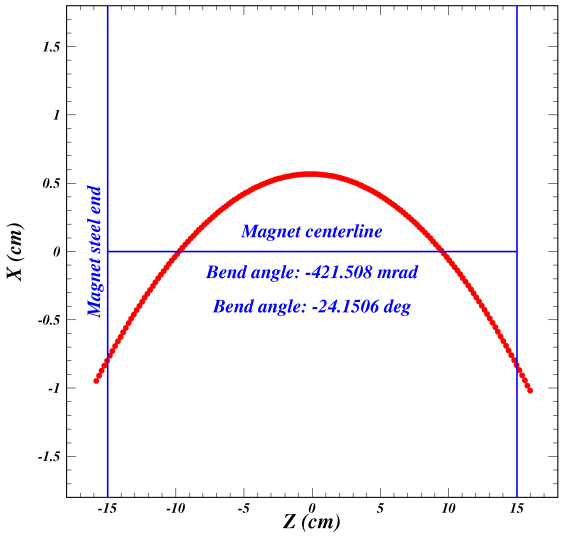

Fig. 4: Overhead view of central trajectory of 150 MeV beam through the R4.BEN03/4 H-dipole.

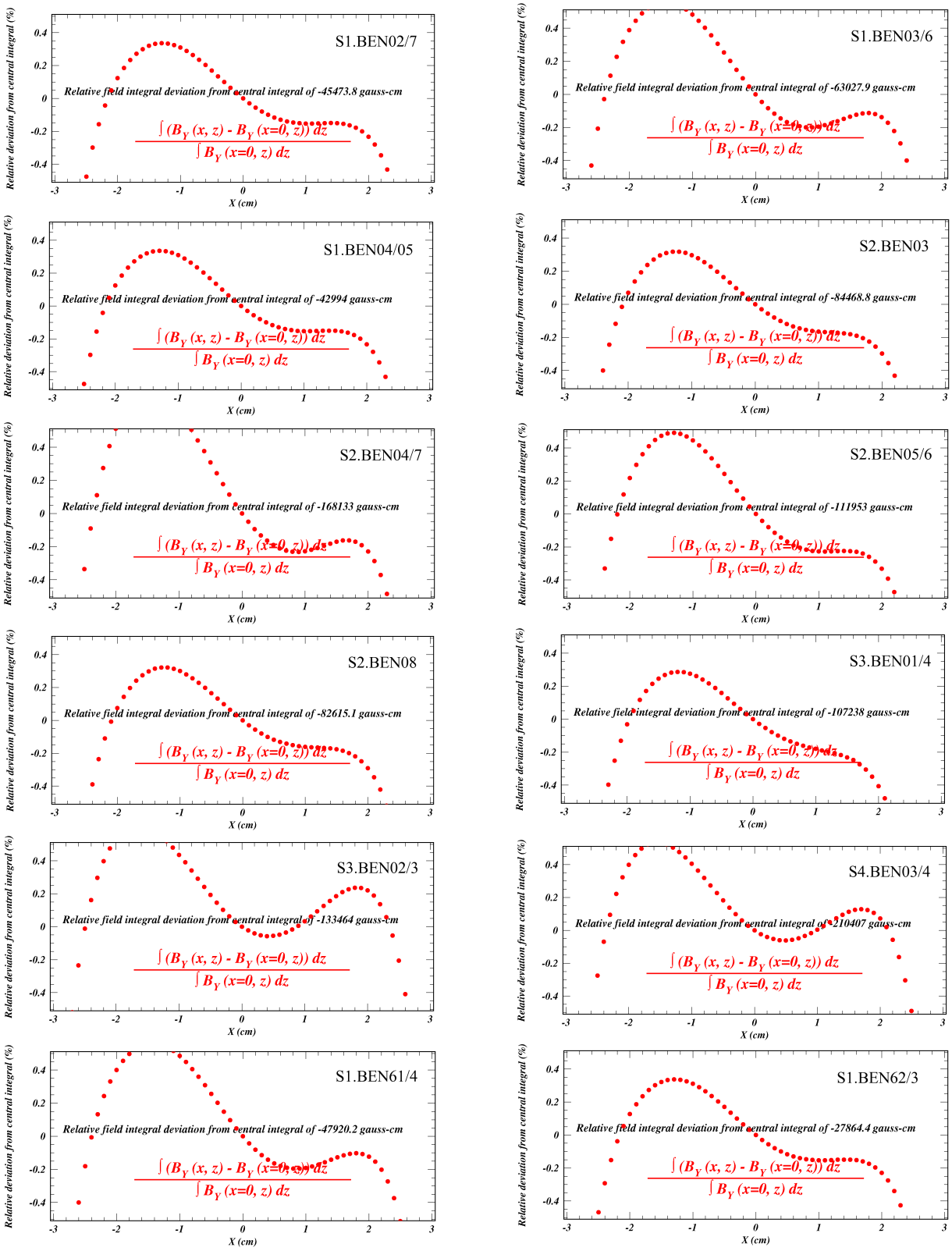

Fig. 5: SX Field Integral Uniformities: Relative deviation (%) from the central integral as a function of location along the transverse axis. The asymmetry about $X = 0$ is a consequence of the asymmetric chamfers

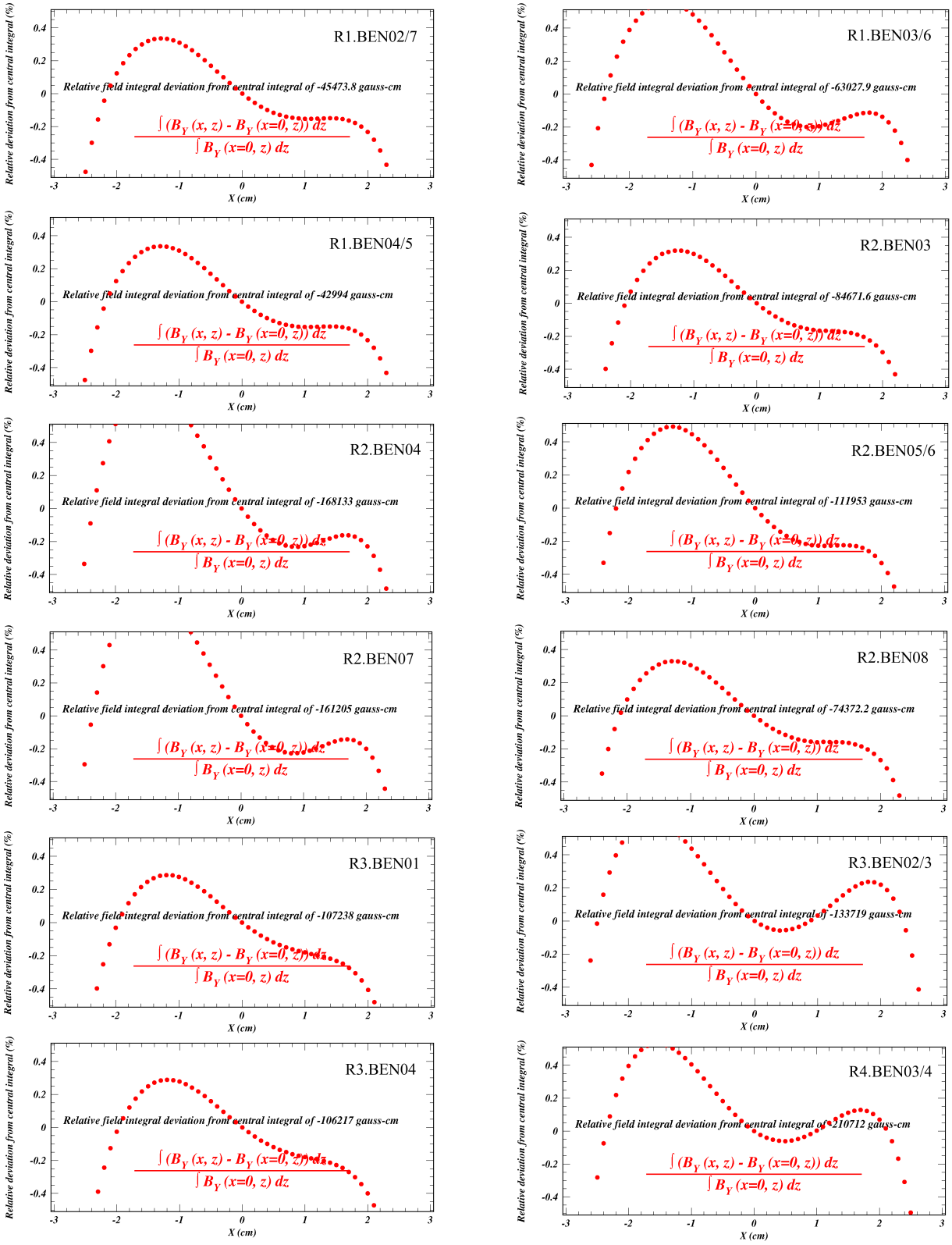

Fig. 6: RX Field Integral Uniformities: Relative deviation (%) from the central field integral as a function of location along the transverse axis. The asymmetry about $X = 0$ is a consequence of the asymmetric chamfers.

2.2 Data Visualization with PAW

Once the tracking data were collected with OPERA, the PAW utility was used for analysis. The beam track through the dipole that achieved the desired bend angle was plotted separately to give a top-down view of how this beam (referred to as the central trajectory) bends through the dipole's magnetic field (see Fig. 4). While this produces a nice visual, it does not reveal much about the dipole's ability to accurately bend beams that are not along the central trajectory. Bend angle uniformity plots, as seen in Figures 7 and 8, show how the bend angle depends on the beam's central position. These plots were used to determine the robustness of the dipole designs: dipoles with large regions of bend angle uniformity will accurately guide beams through the splitter even if the beams are transversely displaced. PAW was also used to visualize the field integral uniformity at the center of the dipoles, which can be seen in Figures 5 and 6. While the field integral uniformities do not determine design quality, they will be useful in performing quality assurance testing at Elytt and Cornell.

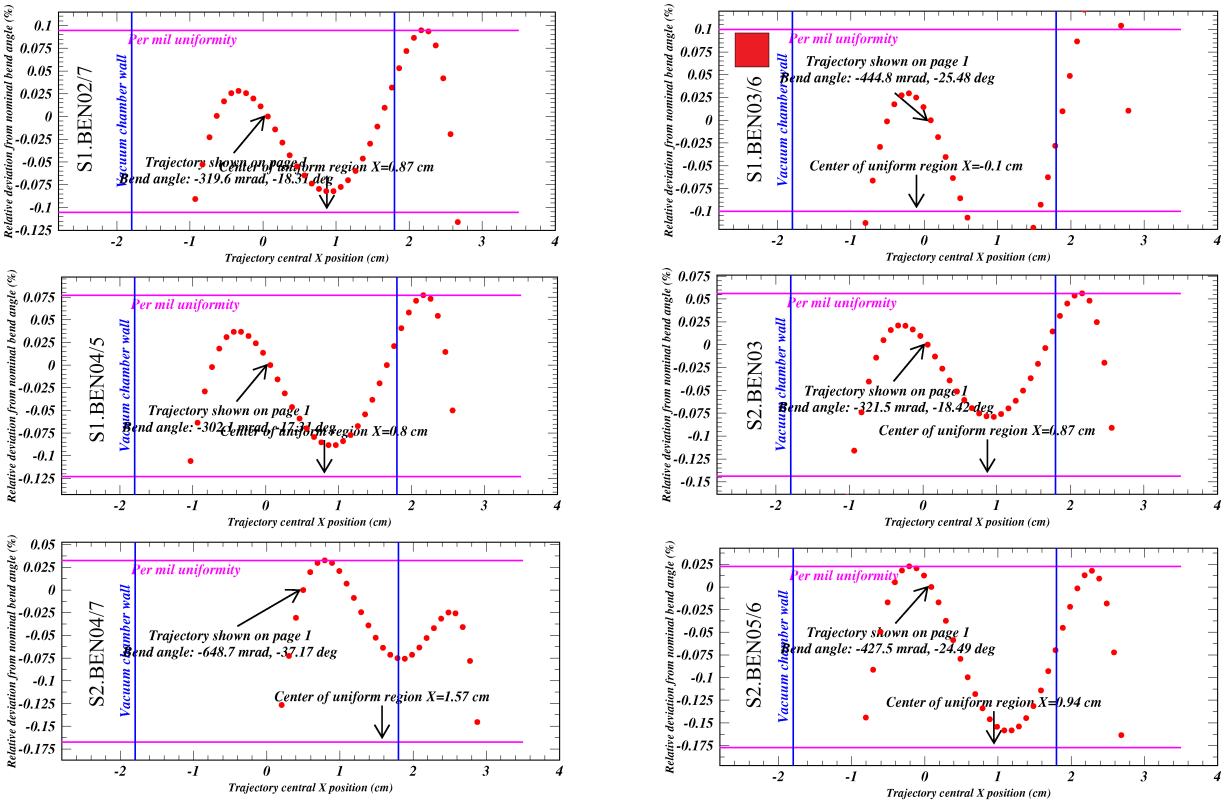

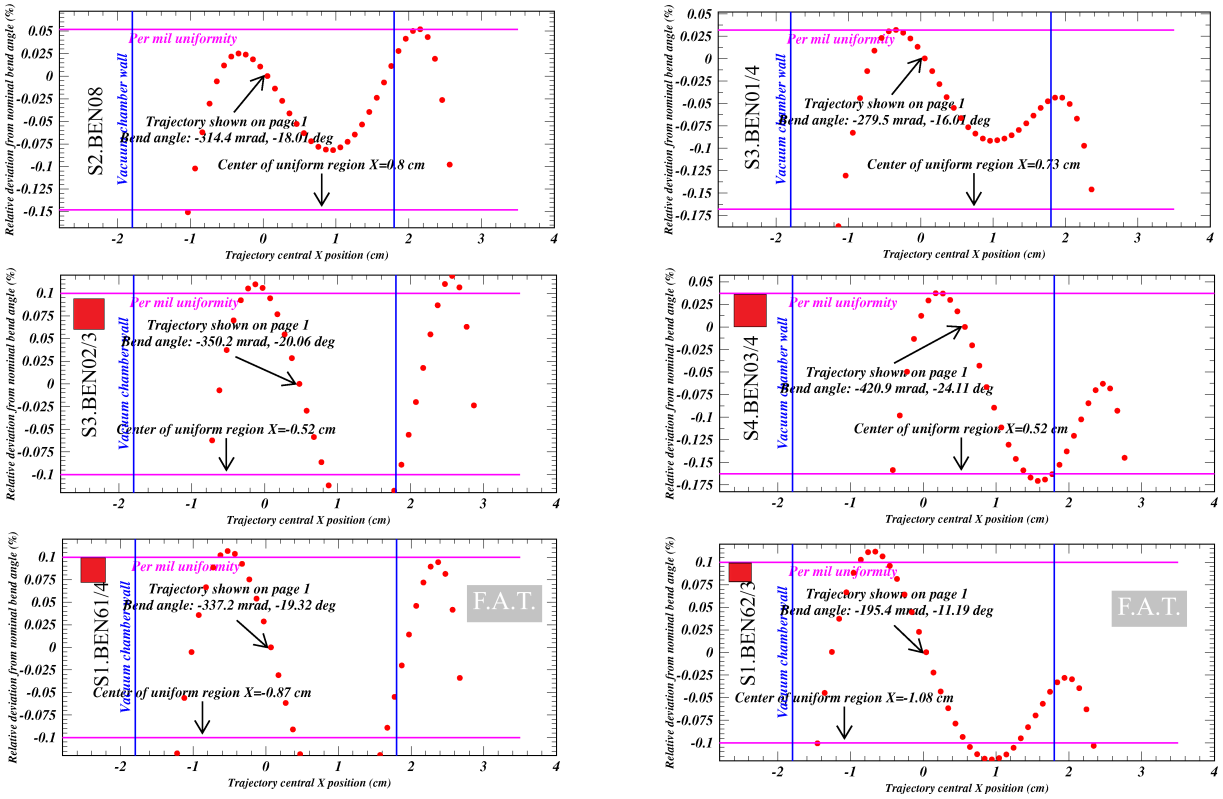

Fig. 7: SX Bend Angle Uniformities: percent deviation from the nominal bend angle as a function of location along the transverse axis. Goal: ±0.1% over 30-mm. Marginally out of spec magnets are identified by a red square.

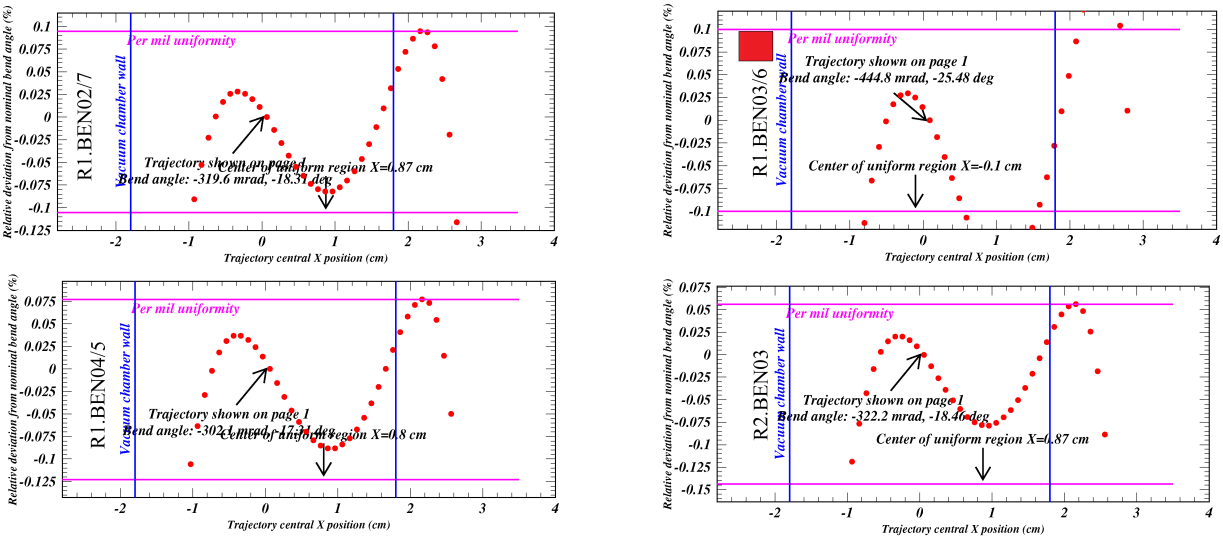

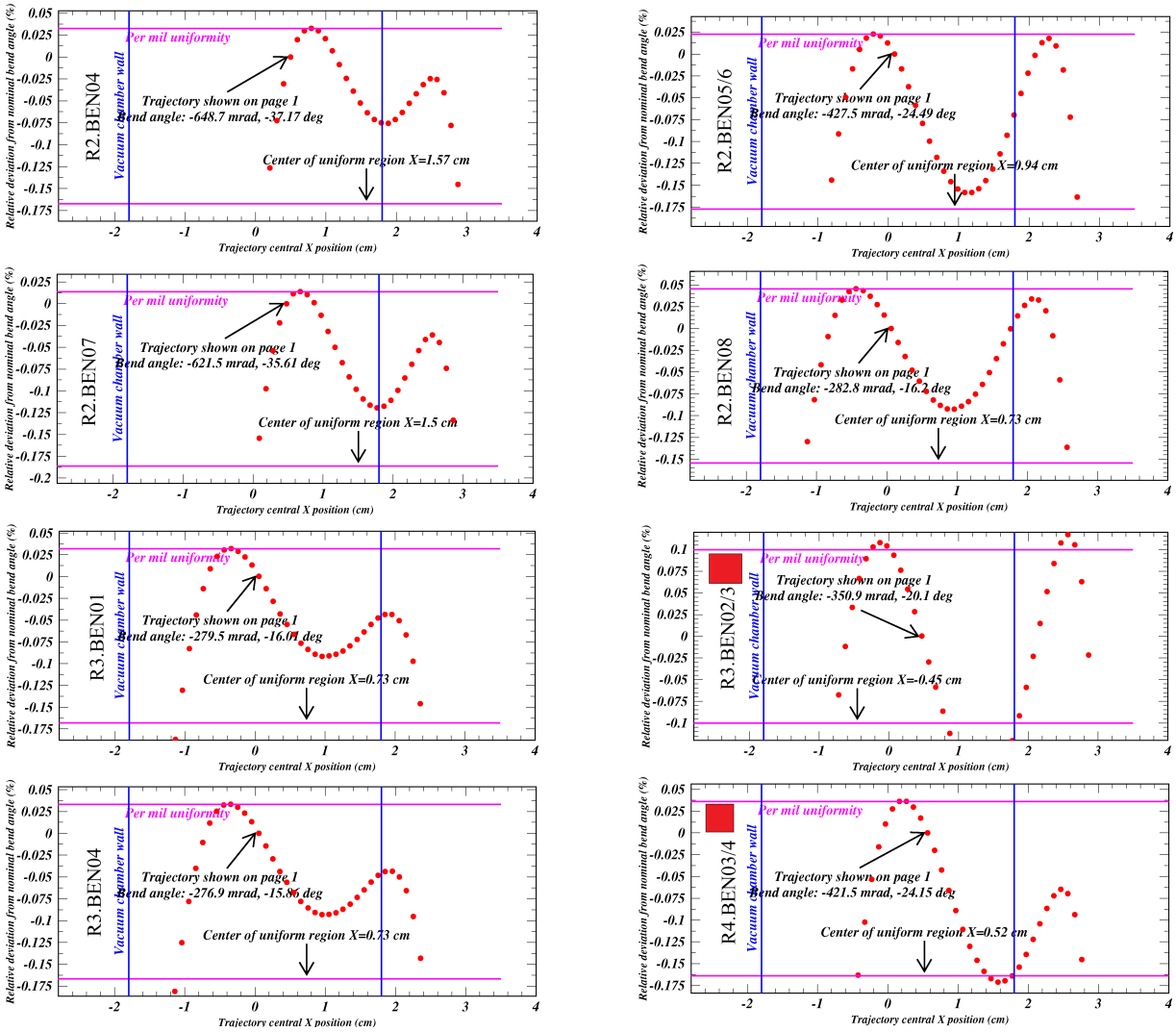

Fig. 8: RX Bend Angle Uniformities: percent deviation from the nominal bend angle as a function of location along the transverse axis. Goal: ±0.1% over 30-mm. Marginally out of spec magnets are identified by a red square. The trajectory with the arrow in the plot for R4.BEN03/4 is shown in Fig 4.

3 H-Dipole Tracking Study Results

Once all magnets were modeled and their data were plotted, analysis of the resulting data began. Special attention was paid to the bend angle uniformity plots (see Figs 7 and 8) during this study. As shown, most magnets achieve ±0.1% uniformity across a 30-mm region. These plots were compared with Elytt's Ansys-produced [1] bend angle uniformity plots, and the two models consistently agreed. This finding indicates that Elytt is capable of producing H-dipoles within specification. Additionally, this study indicates that chamfer designs can be further refined to bring all dipoles within specification. The chamfers are made necessary due to the needed range of excitation of the magnets (up to 7 kG), the transverse space constraints of the splitters (the magnets must be less than 21-cm wide), and by the range

of required bend angles (15 ° to 37 °). The chamfers are used to adjust the field integral on the trajectory and produce different bend angles for magnets with identical steel and coil lengths. For example, there are two chamfer types that are used for the 16-cm-long dipoles; one produces a roughly 16 ° bend while the other guides beams along a sharper 24 ° bend. The excitation current of the dipole further controls the bend angle. Changing the chamfer design at a later date should not negatively impact the arrival of the H-dipoles since the chamfers are machined independently from the dipoles and are intended to be screwed onto the steel on site. Information about the parameters used to build the H-dipole models in OPERA can be found in Table 3.

Table 3: August 7, 2017 - Operational parameters for the CBETA splitter dipole and common Magnets. These values are defined by the lattice design of 10 April 2017. They include the required adjustment margins on the maximum field values of 10%.

Parameter	**H-Dipole 21x31x16**	**H-Dipole 21x31x24**	**H-Dipole 21x31x31**	**Common 34x42x16**
JAC OPERA model version number	33	33	33	39
Number of magnets	24	4	8	4
Gap or Bore (cm)	3.6	3.6	3.6	3.6
Steel height (cm)	30.5	30.5	30.5	42.0
Steel width (cm)	21.0	21.0	21.0	34.0
Steel length (cm)	16.0	24.0	31.0	16.0
Width including coil (cm)	21.0	21.0	21.0	34.0
Length including coil (cm)	24.1	37.4	37.4	24.1
Pole width (cm)	7.66	7.66	7.66	19.66
Field (T)	0.230-0.602	0.623-0.655	0.424-0.670	0.363-0.393
Field Integral (T-m) at X = 0 (1) cm	0.046-0.120	0.177-0.185	0.146-0.231	0.081-0.087
Good Field Region (mm)	± 15	± 15	± 15	± 50
Central Field Uniformity* (%)	± 0.1	± 0.1	± 0.1	± 0.1
Field Integral Uniformity* (%)	± 0.1	± 0.1	± 0.1	± 0.5
Bend Angle Uniformity* (%)	± 0.1	± 0.1	± 0.1	± 0.5
NI per coil (Amp-turns)	3422-8972	9282-9667	6281-9918	5456-5914
Turns per coil	4 x 13	4 x 13	4 x 13	4 x 13
Coil cross section (cm x cm)	2.85 x 10.55	2.85 x 10.55	2.85 x 10.55	2.85 x 10.55
Conductor cross section (cm x cm)	(0.56x0.61)/0.36-cm diam hole			
Conductor straight length (cm)	16.4	29.8	29.8	16.4
Coil inner corner radius (cm)	1.40	0.84	0.84	14.
Conductor length per turn, avg (cm)	59.78	86.4	86.4	69.8
R_{coil} (Ω)	0.0229	0.0330	0.0330	0.267
L (mH)	2 x 10.0 = 20.0	2 x 13.8 = 27.6	2 x 17.0 = 34.0	2 x 23.5 = 47.1
Power supply current (A)	65.8-172.5	178.5-185.9	120.8-190.7	104.9-113.7
Current density (A/mm^2)	2.85-7.46	7.72-8.04	5.22-8.25	4.54-4.92
Voltage drop/magnet (V)	3.0-7.9	11.8-12.3	8.0-12.6	5.6-6.1
Power/magnet (W)	198-1364	2103-2281	963-2401	588-691

* Defined as horizontal deviation from the ideal field $(B_Y - B_Y^{\text{ideal}})/B_Y^{\text{ideal}}$.

3.1 Bend Angle Uniformities

The plots shown in Figures 7 and 8 were the most important component of this study. These images show the percent deviation from the nominal bend angle as a function of the beam's central transverse position for a given magnet. As shown in these figures, the uniformity plots' two peaks are a result of the chamfers. The horizontal pink lines define a region ± 0.1% in width. This defines one of the conditions that was considered when determining if a magnet was within specification: CBETA requires that these H-dipoles have

bend angle uniformities within ±0.1% of the nominal bend angle over a 30-mm region. The horizontal axis was used to measure if the region of uniformity is wide enough. The magnets that failed to have a wide enough region of uniformity or exceeded the ±0.1% specification are marked with a red square. For the most part, the magnets that are marked are barely out of spec, and achieve uniformity within ±0.125% of the nominal bend angle. In these cases, the CBETA and Elytt teams must decide if they want to tweak the chamfer designs in search of tightening the uniformity. The most notably out of spec dipoles are the S1.BEN61 and S1.BEN64 magnets that will be part of next Spring's Fractional Arc Test (FAT). The cause of their poor uniformities will need to be further investigated. The takeaway from these plots is that the majority of H-dipoles have bend angle uniformities that are within (or barely outside of) ±0.1% of the nominal bend angle over a region of 30-mm.

3.2 37° H-Dipoles Require Unique Treatment

The dipoles S2.BEN04, S2.BEN07, R2.BEN04, and R2.BEN07 are responsible for providing a the 78 MeV beam with a 37 ° bend angle. This large bend angle required a unique dipole design solution. Initially, these dipoles were intended to have 31-cm-long steel yokes. However, the models showed that this design was too unstable: the large sagitta resulted in an anomalously high field integral gradient (see Fig. 9). A ten percent change in the activation current greatly impacted the size of the region of bend angle uniformity as well as the bend angle itself (see Fig. 10). While new chamfer designs helped improve the region of bend angle uniformity, these changes were made on the millimeter scale, indicating the 31-cm design was still too sensitive to small changes. This instability led to a new design: the coil for these magnets will remain 31-cm in length, but the steel will be shortened to 24-cm to reduce the sagitta of the trajectory. This solution is advantageous for a couple of reasons. First, changes in excitation current do not severely impact the dipole's performance. Additionally, the shortened steel design results in a field integral gradient similar to those of the other H-dipoles, which implies that this design will behave more like the other dipoles (see Figs 5 and 6).

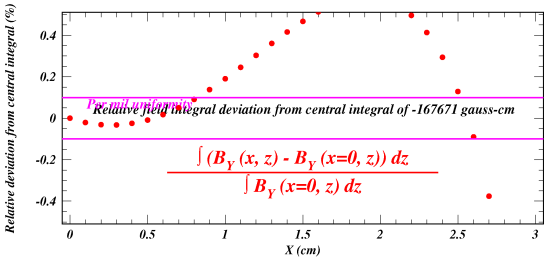

Fig. 9: Field integral uniformity of 31-cm-long S1.BEN04/7 magnets with an excitation current of 7227 amp-turns. Compare this with the right half of the field integral uniformity of the 24-cm-long S1.BEN04/7 dipoles in Figure 5.

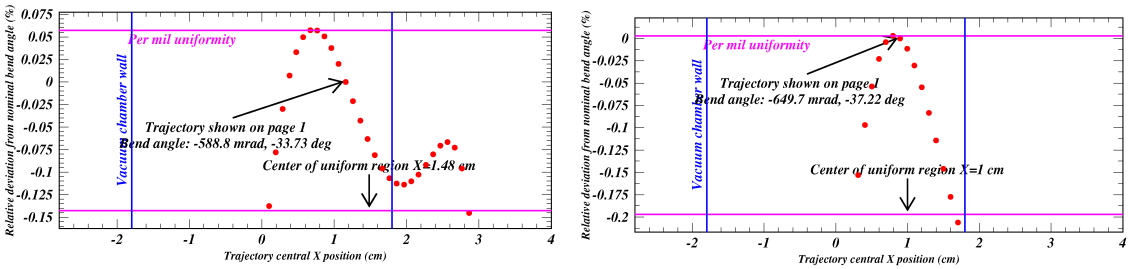

Fig. 10: Bend angle uniformity plots for S1.BEN04/7 with 31-cm-long steel. Left: excitation current is 6570 amp-turns and the bend angle is 33.7 °. Right: excitation current is 7227 amp-turns and the bend angle is 37.2 °. Note that this 10% difference in current impacts the breadth of the uniform region.

3.3 Optimized Magnet Transverse Positions

The centers of regions of bend angle uniformity provide the offset data shown in Table 4. These data are used to make the CBETA layout more accurate and provide better informed insight regarding potential magnet collisions. The offsets will also maximize the region of bend angle uniformity available to the beams once the splitters are constructed.

Table 4: Offset values of SX and RX dipoles derived from bend angle uniformity plots. In cases where the magnet is out of spec, the offset value is calculated manually, as the center of uniformity displayed in Figs 7 and 8 is miscalculated. These values are used to update the CBETA layout.

Dipole	Offset (mm)	Dipole	Offset (mm)	Dipole	Offset (mm)	Dipole	Offset (mm)
S1.BEN02	8.7	S1.BEN03	-10.5	S1.BEN04	8.5	S1.BEN05	8.5
S1.BEN06	-10.5	S1.BEN07	8.7	S2.BEN03	7	S2.BEN04	-15.5
S2.BEN05	9.5	S2.BEN06	9.5	S2.BEN07	-15.5	S2.BEN08	8
S3.BEN01	6	S3.BEN02	-11	S3.BEN03	-11	S3.BEN04	6.5
S4.BEN03	-11.5	S4.BEN04	-11.5	–	–	–	–
S1.BEN63	-8	S1.BEN64	-8	S1.BEN61	-8	S1.BEN62	4
R1.BEN02	8.7	R1.BEN03	-10.5	R1.BEN04	8.5	R1.BEN05	8.5
R1.BEN06	-10.5	R1.BEN07	8.7	R2.BEN03	9	R2.BEN04	-15.5
R2.BEN05	9.5	R2.BEN06	9.5	R2.BEN07	-15	R2.BEN08	7
R3.BEN01	6.5	R3.BEN02	-11	R3.BEN03	-11	R3.BEN04	6.5
R4.BEN03	-12	R4.BEN04	-12	–	–	–	–

3.4 Tracking Study Summary

This tracking study relied on careful magnet modeling and analysis of the resulting data. Optimizing magnet performance must be balanced with space constraints of the splitter regions. The results of this study and the steps being taken as a result of it take into account this need for balance. These same concerns are guiding the design process of the common dipoles.

4 Ongoing Work: Common Magnets

Despite their name, the common dipoles are unique in that they are responsible for transitioning four beams into and from their respective beam pipes in the splitter regions. The S1.BEN01 common magnet also has a size constraint imposed by the location of a nearby beam dump pipe (see Fig 13). Another design challenge is that the beam offsets are different for the two ends of the splitters; the transverse displacement between the 42 and 150 MeV beams at the magnet center in S1.BEN01 and R1.BEN01 is about 8 mm, while the displacement is about 41 mm in the other two common magnet locations (see Fig. 12). These displacements help set the requirements for a good field region, which is much wider than that needed for the H-dipoles. Setting the offsets for these magnets is more complicated than for the H-dipoles because these magnets must accurately guide multiple beams. When determining the needed offset, one must consider where the magnet can go such that all four beams are within their individual regions of uniformity (see Figs 14 and 15). If the magnet were only offset to optimize the bend angle uniformity of one beam, other beams may be placed in regions where they will bend too much or not enough. Additionally, the offset of the magnet must take into account the offset needed relative to the horizontal axis shown in Figures 14 and 15 as well as the offset relative to the global coordinate system of the accelerator. At the time of writing, the total offset for the S1.BEN01 magnet has been set as -0.1473 cm in the global X direction. This places the 42 MeV beam at X = 3.5 cm and the 150 MeV beam at X = 2.7 cm in the local coordinates defined in Figure 12. The offset values for the other magnets are pending.

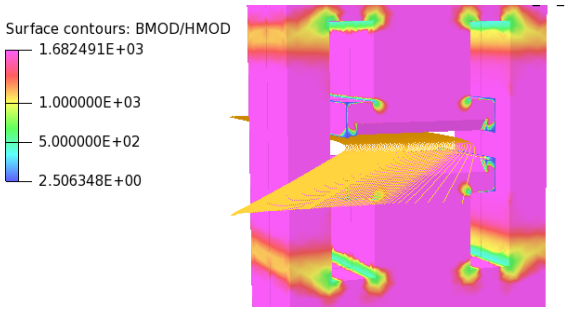

Fig. 11: Common Dipole design with beam tracking for 42 MeV electrons. Notice the wide poleface and narrow pole; this design element is permissible because the field range for these magnets is only 0.34-0.37 T. A simple symmetric chamfer is used to improve the field integral gradient. These design elements are unique among the dipoles used in CBETA.

Work on a design that will function in all four locations is currently underway (see Fig. 11). This design is different from the other dipoles, as it has a pole that extends under the coils. This increases the area of the pole that the beam pipe passes through without using as much steel as would be required for a pole of a single width. This design is based after the design that will be used for the splitter quadrupole magnets. A simple symmetric chamfer helps extend the length of the uniform bend angle region of the beams as well. As the design stands, the S1.BEN01 magnet will clear the dump line by 10 mm without cutting it, and the good field region can be extended by an additional 20 mm if its corner is cut. In collaboration with Elytt Energy, refinements to the design will continue until a satisfactorily robust magnet is achieved. Information about the parameters used in the OPERA model of these magnets can be found in Table 3.

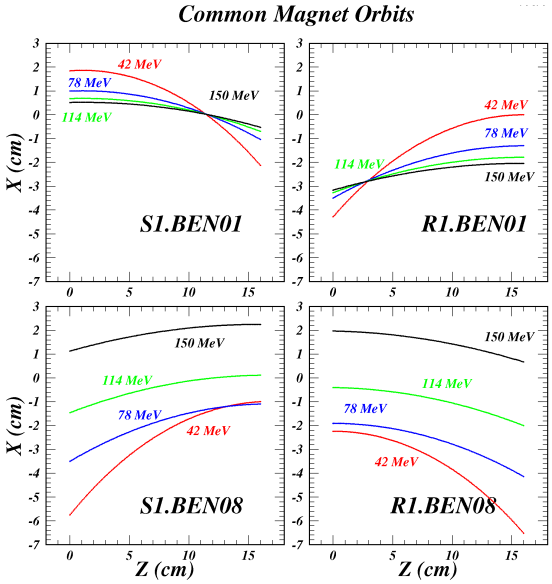

Fig. 12: Beam orbits through common magnet in each location. The X axis is relative to the center of the beam pipe after the magnet is rotated. The difference in transverse displacement between 42 and 150 MeV beams in the top and bottom rows highlights one of the challenges that these magnets must overcome. The center of the magnet along the horizontal axis is at $Z = 8$ cm. [2]

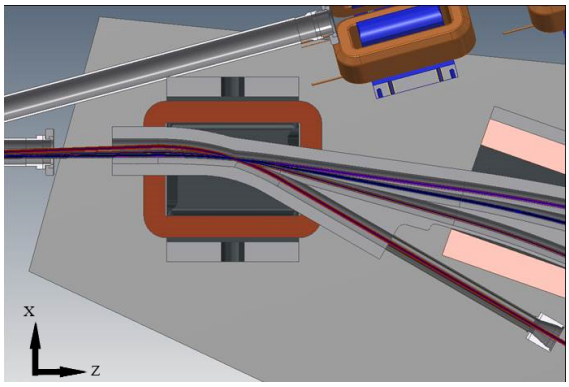

Fig. 13: S1.BEN01 and nearby dump pipe for 6 MeV beams. This pipe constrains the size/position of the S1.BEN01 magnet. This image is with respect to the accelerator's global coordinates. All common magnets will be aligned such that their faces are perpendicular to the beams as they enter, in the case of S1.BEN01 and R1.BEN08, or exit, as with S1.BEN08 and R1.BEN01. [2]

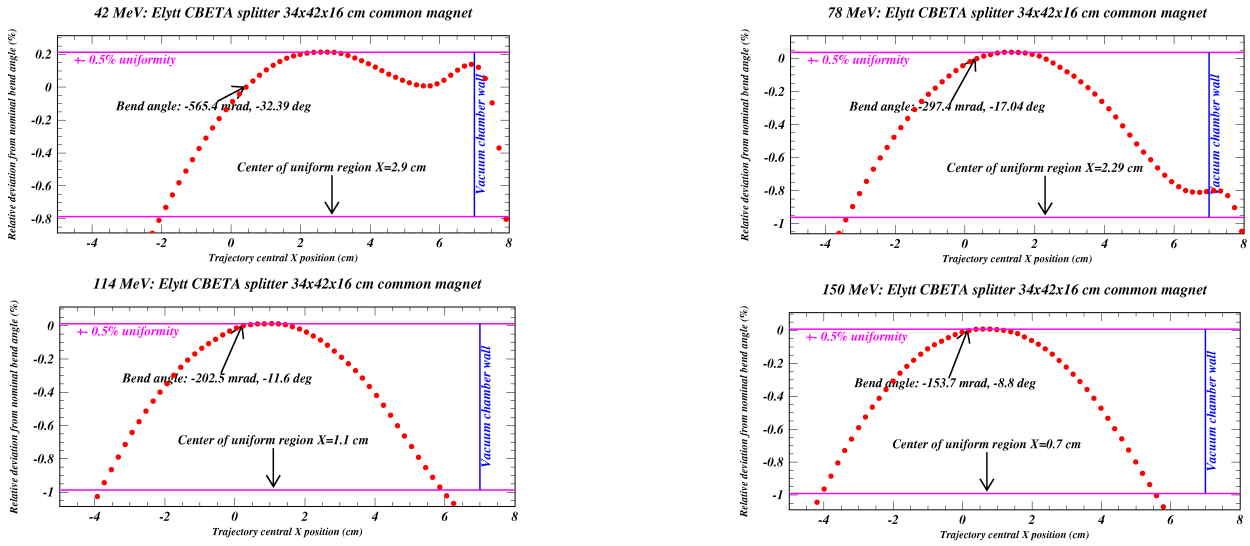

Fig. 14: Bend angle uniformities for S1.BEN08 and R1.BEN01 common magnets. The beams exit these magnets in parallel. Unlike the H-dipoles, the region of uniformity is defined as being within $\pm 0.5\%$ of the nominal bend angle. Due to the different widths of the beams' regions of uniformity, more consideration must be taken when determining the offset.

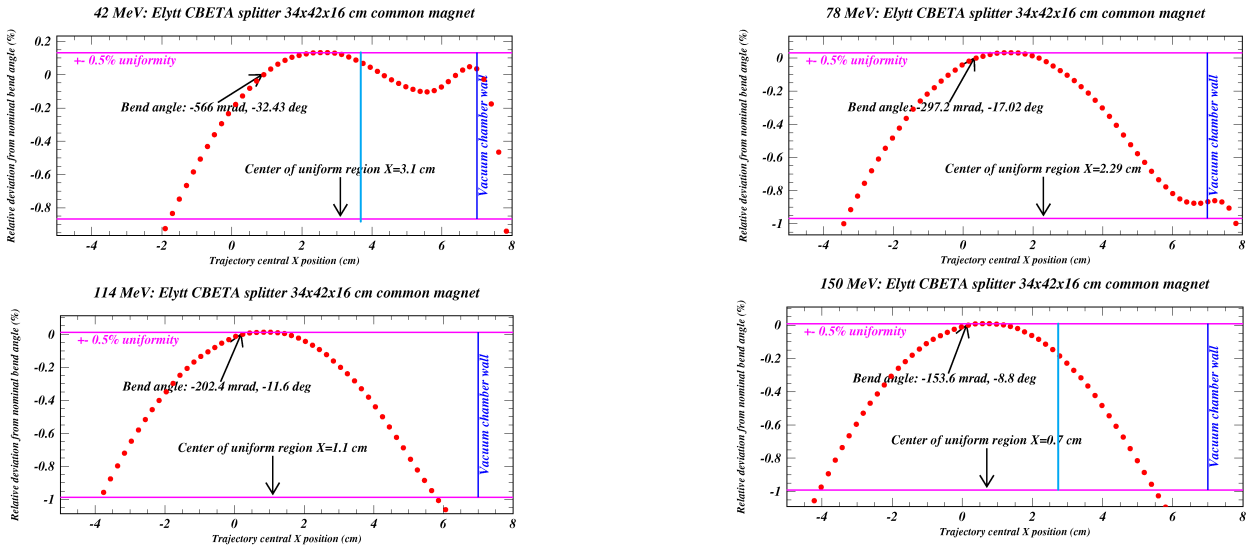

Fig. 15: Bend angle uniformities for S1.BEN01 and R1.BEN08 common magnets. The beams enter these magnets in parallel. Unlike the H-dipoles, the region of uniformity is defined as being within ±0.5% of the nominal bend angle. Due to the different widths of the beams' regions of uniformity, more consideration must be taken when determining the offset. The necessary transverse offset for these magnets in their local coordinates (shown here) is marked by a blue line on the 42 and 150 MeV plots. The beam dump pipe near S1.BEN01 must also be considered when offsetting this magnet.

5 Conclusion

This summer saw the completion of tracking studies of the 36 splitter H-dipoles; the finalization of the dipoles' designs; and the beginning of the design of the four common magnets. The tracking study showed that Elytt is capable of producing H-dipoles that have bend angle uniformities within ± 0.1% of the nominal bend angle across a 30-mm region. These studies also indicated that removable chamfers allow for fine tuning of the trajectory field integrals without needing to change the shape of the magnet steel itself. The 37 ° H-dipoles showed that shortening steel is another dipole design option that can improve magnet performance. Finally, the completion of the tracking study of the H-dipoles provided necessary offset values that are used in models of the splitter layout and will be used in assembling the splitters themselves.The insights gained from the tracking study of the H-Dipoles will help inform the design of the common dipoles, and will help produce robust and successful magnets.

The H-dipoles needed for the FAT are scheduled to arrive in late November of this year. Elytt has indicated confidence that it will be able to deliver the two common magnets needed for the FAT in time, with arrival expected in early 2018. The confidence gained from this study helps assure that, once completed, CBETA will be a successful contribution to accelerator science.

Acknowledgments

I would like to thank my mentor Jim Crittenden for his guidance and advice this summer. I would also like to thank Karl Smolenski for his encouragement. This research would not be possible without the generosity of the National Science Foundation and the Cornell Laboratory for Accelerator-Based Sciences and Education.

References

[1] *Ansys Simulation Software*. Ansys Group. URL: `www.ansys.com`.

[2] J.A. Crittenden. *Splitter Common Magnet Design Issues*. Powerpoint.

[3] *Opera Simulation Software*. Cobham Group. URL: `www.operafea.com`.

[4] *Physics Analysis Workstation*. CERN. URL: `paw.web.cern.ch/paw`.

[5] Richard Ryan. *CBETA Science*. URL: `https://www.classe.cornell.edu/Research/CBETA/CBETAScience.html`.

[6] N. Banerjee *et al. Draft CBETA Design Report*. Ed. by G. Hoffstaetetter and D. Trbojevic.